Is intranasal administration an opportunity for direct brain delivery of lacosamide?

Joana Gonçalves , Gilberto Alves , Carla Fonseca , Andreia Carona , Joana Bicker , Amílcar Falcão , Ana Fortuna

PII: S0928-0987(20)30420-6
DOI: https://doi.org/10.1016/j.ejps.2020.105632
Reference: PHASCI 105632

To appear in: *European Journal of Pharmaceutical Sciences*

Received date: 10 September 2020
Revised date: 20 October 2020
Accepted date: 26 October 2020

Please cite this article as: Joana Gonçalves , Gilberto Alves , Carla Fonseca , Andreia Carona , Joana Bicker , Amílcar Falcão , Ana Fortuna , Is intranasal administration an opportunity for direct brain delivery of lacosamide?, *European Journal of Pharmaceutical Sciences* (2020), doi: https://doi.org/10.1016/j.ejps.2020.105632

Highlights:

- The first *in vivo* pharmacokinetic study of lacosamide after intranasal administration.
- Lacosamide intranasal administration enables direct nose-to-brain drug delivery.
- The *in situ* nasal gel has no impact on nasal and lung cells viability.
- Drug target efficiency (DTE) was 128.6% in the brain.

Title

Is intranasal administration an opportunity for direct brain delivery of lacosamide?

Author names and affiliations

Joana Gonçalves[a,b], Gilberto Alves[c], Carla Fonseca [a], Andreia Carona[a,b], Joana Bicker[a,b], Amílcar Falcão[a,b], Ana Fortuna[a,b*]

[a] Faculty of Pharmacy, University of Coimbra, Coimbra, Portugal;

[b] Coimbra Institute for Biomedical Imaging and Translational Research, University of Coimbra, Coimbra, Portugal;

[c] CICS-UBI – Health Sciences Research Centre, University of Beira Interior, Covilhã, Portugal.

*** Corresponding author**

Ana Fortuna, PharmD, Ph.D

Faculty of Pharmacy, University of Coimbra

Pólo das Ciências da Saúde, Azinhaga de Santa Comba

3000-548 Coimbra, Portugal

Phone: +351 239488400 / Fax: +351 239488503

E-mails: afortuna@ff.uc.pt | anacfortuna@gmail.com

Abstract

Lacosamide is well-known as an effective and safe anticonvulsant drug. Nevertheless, there are also evidence of anti-epileptogenic, neuroprotective and antinociceptive properties of lacosamide. It is currently available as oral and intravenous (IV) formulations, and its brain concentrations and therapeutic effect depend on its passage across the blood-brain barrier (BBB). Therefore, to circumvent the restrictive BBB, we herein evaluated the intranasal (IN) administration of lacosamide.

Nasal thermoreversible gels were screened *in vitro* for their influence on the viability of human nasal septum (RPMI 2650) and lung adenocarcinoma (Calu-3) cells. According to the Alamar Blue test, the *in situ* gel composed of Pluronic F-127 (22.5%, w/v) and Carbopol 974P (0.2%, w/v) did not affect cell viability, which remained higher than 85%, within the concentration range of lacosamide.

The *in situ* gel was intranasally administered to healthy male CD-1 mice (8.33 mg/kg) to describe the pharmacokinetic profiles of lacosamide in plasma, brain, lung and kidney and compare them with those obtained after IV administration of the same dose.

Accordingly, IN administration allowed a fast (t_{max} in plasma: 5 min) and complete systemic absorption of lacosamide (bioavailability: 120.46%). Interestingly, IN lacosamide demonstrated higher exposure (given by the AUC_t) in the brain (425.44 µg.min/mL *versus* 274.49 µg.min/mL), but lower exposure in kidneys (357.56 µg.min/mL *versus* 762.61 µg.min/mL), in comparison to IV administration. These findings, together with the t_{max} in brain of 15 min, a drug targeting efficiency (DTE) of 128.67% and a direct transport percentage of 22.28%, evidence that part of lacosamide reaches the brain directly after nasal administration, even though penetration into the brain from the systemic circulation seems to be the major determinant of brain exposure. Importantly, lacosamide concentrations found in lungs following IN administration were considerably higher than those observed after IV injection, until 30 min post-dosing ($p < 0.05$). Nevertheless, attained drug concentrations were lower than those tested *in vitro* in the Calu-3 cell line (1-100 µM), indicating that adverse effects are unlikely to occur *in vivo*.

Hence, it seems that the proposed IN route has potential to be a suitable and valuable strategy for the brain delivery of lacosamide in emergency conditions and for the chronic treatment of epilepsy and other neurological diseases.

Keywords

Lacosamide; Intranasal administration; Nose-to-brain delivery; Pharmacokinetics; Refractory epilepsy

Abbreviations

AEDs, antiepileptic drugs; AUC, area under the concentration-time curve; AUC_t, area under the concentration-time curve from time zero to the time of last measurable concentration; AUC_{extrap}, extrapolated area under the concentration-time curve; AUC_{inf}, area under the concentration-time curve from time zero to infinity; BBB, blood-brain barrier; $B_{brainIN/IV}$, brain bioavailability between IN and IV routes; C_{max}, maximum concentration; CNS, central nervous system; CYP, cytochrome P450; CV, coefficient of variation; LLOQ, lower limit of quantification; DRE, drug-resistant epilepsy; DTE, drug targeting efficiency; DTP, direct transport percentage; F_{Abs}, absolute bioavailability; HPLC, high performance liquid chromatography; IN, intranasal; IV, intravenous; P-gp, P-glycoprotein; $t_{1/2}$, half-life; t_{max}, time to reach the C_{max}; SD, standard deviation; SEM, standard error of the mean; VGSC, voltage-gated sodium channels

1. Introduction

Lacosamide is unique among all marketed antiepileptic drugs (AEDs) due to its two novel mechanisms of action and favorable pharmacokinetic and safety profiles. It selectively enhances the slow inactivation of voltage-gated sodium channels (VGSCs), in opposition to classic VGSC modulators, such as carbamazepine, phenytoin and oxcarbazepine, which increase fast channel inactivation (de Biase et al., 2014). The slow inactivation of VGSCs is an endogenous mechanism by which neurons reduce ectopic hyperactivity and their modulation by lacosamide stabilizes hyper-excitable neuronal membranes in a selective manner, decreasing repetitive neuronal firing. Hence, lacosamide reduces the pathophysiological hyperactivity underlying epilepsy without affecting the physiological activity (Halford and Lapointe, 2009). In addition, lacosamide inhibits a nervous system phosphoprotein called collapsing-response mediator protein-2, attenuating the effects of neurotrophic factors on axon outgrowth and suppressing spontaneous recurrent seizures, with consequent inhibition of epileptogenesis (Wang et al., 2018). This feature is unique to lacosamide, as the other AEDs lack it (Engel and Pitkänen, 2020).

The aforementioned mechanism of action confers lacosamide fewer adverse effects and an excellent therapeutic profile, achieving patients high rates of seizure freedom, in monotherapy or as add-on treatment of partial-onset seizures, with or without secondary generalization (de Biase et al., 2014; Halford and Lapointe, 2009). Its multifactorial mechanism of action created the possibility of using lacosamide in other pathologies, mainly due to its antinociceptive and neuroprotective functions, specifically chronic migraine treatment (Lionetto et al., 2012), glioma (Rizzo et al., 2017), hypoxic-ischemic brain injury due to its neuroprotective effect (Kim et al., 2017) and in diabetic patients with neuropathic pain (Carmland et al., 2019; Moutal et al., 2016) and inflammation (Al-Massri et al., 2018).

Lacosamide is also distinctive among other AEDs because it exhibits many of the pharmacokinetic characteristics of an ideal AED. It displays a dose-proportional pharmacokinetic profile, rapid and complete intestinal absorption, low plasma protein

binding (< 15%) and minor first-pass hepatic metabolism. Nevertheless, it is a P-glycoprotein (P-gp) substrate (Zhang et al., 2013), which is overexpressed in refractory epilepsy (Lazarowski et al., 2007; Leandro et al., 2019). Consequently, it is expected that the quantity of lacosamide that can cross the BBB decreases as the disease advances and the P-gp expression enhances. Furthermore, only 40% of the administered dose is excreted as the unchanged form. The remaining dose is previously metabolized to the inactive *O*-desmethylmetabolite that results primarily from cytochrome P450 (CYP) 2C19 activity, and to other minor metabolites that result from CYP2C9 and CYP3A4 mediated metabolism. Consequently, the concomitant use of lacosamide with CYP2C19 substrates or inhibitors may decrease the formation of the major metabolite by approximately 60%, increasing the risk of toxicity (Cawello et al., 2014). Inter-individual variability has also been observed due to the polymorphic alleles that encode CYP2C19 (de Biase et al., 2014). Accordingly, the renal excretion of *O*-desmethylmetabolite decreases 70% in poor metabolizers relatively to extensive metabolizers (Dean, 2018). Since both unchanged form and metabolites of lacosamide are excreted in urine, dose adjustment is required for patients with severe renal impairment and submitted to hemodialysis, which removes approximately 50% of the drug from plasma (Cawello et al., 2013). Indeed, the half-life ($t_{1/2}$) of lacosamide increases from 13h in healthy individuals to up to 18-20 h in severe renal impaired patients, compromising the drug's safety profile (Cawello et al., 2013; Kumar et al., 2017).

Besides the aforementioned advantages of lacosamide, it is currently available in different dosage forms, including syrup and tablets for oral administration, and solution for IV infusion; these pharmaceutical formulations are bioequivalent and directly converted without dose adjustment (de Biase et al., 2014). Parenteral administration is beneficial to patients in emergency situations or unable to take oral medications. For instance, we highlight the hospitalized patients, after surgical procedures, patients with swallowing difficulty or suffering from acute gastrointestinal disorders, which is one of the most frequent adverse effect of lacosamide (Halford and Lapointe, 2009). However, IV injection is invasive and requires qualified clinical professionals.

Since ambulatory monitoring systems are being developed to improve seizure detection, novel therapeutic systems must be able to be self-administered "at home" to improve the quality of life of patients with epilepsy and their families (Amengual-Gual et al., 2019). In this context, we developed the present work in order to administer lacosamide by non-invasive intranasal (IN) route. This route is characterized by a fast onset of action and direct nose-to-brain delivery, which results in lower systemic and peripheral exposure than classical drug administration routes. We expect to contribute to the development of a new therapeutic strategy for epilepsy and other neurological diseases, by surpassing hepatic first-pass metabolism and consequently

reducing metabolic drug-drug interactions and the inter-individual variability of the marketed formulations (Gonçalves et al., 2020; Gonçalves et al., 2019). Moreover, as lower plasma concentrations are expected to be attained, systemic side effects, including the renal ones, will be probably decreased. Nevertheless, there is risk of increased drug exposure in lungs and therefore will be herein investigated. Complementarily, the direct nose-to-brain delivery is expected to decrease the development of pharmacoresistance associated to the P-gp overexpression at the endothelial cells of the blood-brain barrier (BBB) (Wang et al., 2016). Therefore, a pharmacokinetic study was performed in mice to compare the biodisposition of lacosamide after IN and IV administrations. Taking into consideration the fast mucociliary clearance in nasal mucosa, lacosamide was loaded into an *in situ* mucoadhesive gel system before being administered in the nasal cavity.

2. Material and methods

2.1. Chemicals and reagents

Lacosamide (Vimpat® solution for infusion, 10mg/mL), used in *in vivo* studies, as well as ketamine (Imalgene® 1000, 100 mg/mL) and xylazine (Vetaxilaze 20®, 20 mg/ml) used for animal anesthesia, were commercially acquired. Antipyrine, applied as internal standard (IS) in the high performance liquid chromatography (HPLC) method, was obtained from Sigma-Aldrich (St. Louis, MO, USA). Lacosamide power (purity > 98%), used for the development and validation of the HPLC method, and *in vitro* studies, was purchased from Molekula SRL (Rimini, Italy).

For the preparation of the *in situ* gel, Pluronic F-127 was purchased from Sigma–Aldrich (St. Louis, MO, USA), while Noveon® Polycarbophil and Carbopol® 974P were acquired from Lubrizol (Wickliffe, OH, USA). Sodium dihydrogen phosphate dehydrate, disodium hydrogen phosphate dehydrate and hydrochloric acid 37%, used to prepare the 0.1 M sodium phosphate buffer pH 5.0, were purchased from Merck KGaA (Darmstadt, Germany).

The preparation of *in vivo* samples and analysis by HPLC required ethyl acetate, methanol and acetonitrile, which were purchased from Fisher Scientific (Leicestershire, UK) and ultrapure water (HPLC grade, 18.2 MΩ.cm) prepared using a Milli-Q Millipore Water Appliance (Milford, MA, USA). Dimethyl sulfoxide (DMSO) used in *in vitro* assays was purchased from Fisher Scientific (Leicestershire, UK). Sodium chloride 0.9% solution was acquired from B. Braun Medical (Queluz de Baixo, Portugal). All the remaining chemicals were obtained from Sigma-Aldrich (St. Louis, MO, USA) unless otherwise stated.

2.2. Preparation of lacosamide formulations

The *in situ* nasal mucoadhesive gel system was developed by the cold method, dissolving Pluronic F-127 in 10 mL of cold Milli-Q water (22.5%, w/v), under magnetic stirring, at a controlled temperature (5- 10°C). After mixture at 4°C overnight, distinct mucoadhesive polymers were tested, particularly Carbopol® 974P and Noveon® Polycarbophil, at different percentages. The one with lower effect on cell viability was selected for *in vivo* pharmacokinetic studies. Therefore, to load lacosamide into the gel, 500 µL of the Vimpat® solution for injection (10 mg/mL) were added to 500 µL of gel, obtaining a final concentration of 5 mg/mL.
The IV solution injected to mice was prepared by diluting Vimpat® 10 mg/mL in saline solution (0.9% NaCl), attaining a final concentration of 2.0825 mg/mL.

2.3. *In vitro* cell viability assays in RPMI 2650 and Calu-3 cell lines

The Alamar Blue assay was performed on the human nasal septum cell line (RPMI-2650, ECACC 88031602) and in human lung adenocarcinoma cell line (Calu-3, ATCC® HTB-55TM) to assess the impact of free lacosamide and distinct mucoadhesive gels on metabolic activity and cell viability. Accordingly, resazurin (7-hydroxy-10-oxophenoxazin-10-ium-3-one), which has high membrane permeability, exists in its oxidized non-fluorescent blue form. Once inside the cells, it is reduced to resorufin by the activity of mitochondrial and cytoplasmic enzymes. Resorufin is a pink substance that emits fluorescence, allowing its quantification and further correlation with viable and metabolic active cells (Page et al., 1993; Rampersad, 2012).

RPMI-2650 cells were cultured in T-75 flasks with Eagle's Minimum Essential Medium (EMEM), supplemented with 2 mM glutamine, 1% nonessential amino acids and 10% inactivated fetal bovine serum (FBS). A 1% penicillin-streptomycin mixture was further added as recommended for bacterial contamination prophylaxis. Calu-3 cells were cultured in the same aforementioned conditions, but making use of Dulbecco's Modified Eagle Medium (DMEM), supplemented with 0.04 M sodium bicarbonate, 1% mixture penicillin-streptomycin and 10% FBS. Three times a week, cells from both cell lines were passed with a 0.25% trypsin-EDTA solution and cultured at 37 °C in 5% CO_2 and 95% relative humidity.

The Alamar Blue assay was conducted as previously described (Gonçalves et al., 2019). Briefly, 3 x 10^5 cells per well (RPMI 2650) or 3.5 × 10^4 cells per well (Calu-3) were seeded in 96-well plates, incubated at 37 °C and 5% CO_2 for 24 h. Once confluent, the cells were treated with 200 µL of each lacosamide solution or empty and drug loaded thermogels for 24 h. Free lacosamide was tested at several concentrations (1, 5, 10, 25, 50, 100, 150, 200, 250 and 400 µM) and distinct thermoreversible gel formulations were tested: with no lacosamide, and loading lacosamide at 50, 100, 150, 200, 250 and

400 µM. Controls corresponding to 100% viability were performed by incubating the cells with fresh medium. Afterwards, treatment solutions were removed, 10% resazurin solution (125 mg/mL) was added and the cells were incubated at 37 °C in 5% CO_2. The incubation period with resazurin was 2 and 3 h for RMPI-2650 and Calu-3 cells, respectively. Finally, fluorescence was determined at 560 and 590 nm in a Biotek Synergy HT microplate reader (Biotek Instruments®, Winooski, VT, USA).

Cell viability was calculated based on the following equation (Gonçalves et al., 2020; Gonçalves et al., 2019):

$$Cell\ viability\ (\%) = \frac{FL_T - FL_W}{FL_{Control} - FL_W}\ x\ 100$$

where FL_T refers to the mean fluorescence observed after incubation with a treatment solution, $FL_{Control}$ is the mean fluorescence observed in non-treated cells and FL_W is the mean fluorescence observed in wells without cells (negative control) (Zachari et al., 2013).

Graphpad Prism® 5.03 software (San Diego, CA, USA) was used for processing *in vitro* data, expressing them as mean ± standard deviation (SD). ANOVA test was applied to determine differences in cell viability treated with lacosamide and gel formulations in relation to the control (100% viability).

2.4. *In vivo* studies

2.4.1. Animals and ethics

All experiments were conducted in accordance with the European Directive regarding the protection of laboratory animals used for scientific purposes (2010/63/EU) (European Parliament, Council of the European Union, 2010) and the Portuguese law on animal welfare (Decree-Law no. 113/2013). The applied experimental procedures were authorized by DGAV – *Direção Geral de Alimentação e Veterinária*.

Healthy adult male CD-1 mice, weighting 25-30 g and supplied by Charles River Laboratories (France), were housed in the local animal facilities under controlled environmental conditions (temperature 20±2°C; relative humidity 55±5%; 12 h light/dark cycle) for at least 1 week before starting the experimental procedures. Before and during the experimental procedures, animals had *ad libitum* access to tap water and standard rodent diet (4RF21, Mucedola®, Italy).

2.4.2. *In vivo* pharmacokinetic study

Mice were randomly divided into two groups, one of which was administered with a single dose of lacosamide by IN route, and the other by IV injection. Before IN or IV administration, animals were anesthetized with a mixture of ketamine and xylazine (100 mg/kg and 10 mg/kg, respectively), by intraperitoneal route, and kept in a properly warmed environment until recovery.

The *in situ* IN gel (50 µL) was administered with a polyurethane tube (24 G, 19 mm) coupled to a 1 mL syringe, introduced about 1 cm from the left nostril of the animal, positioned laterally. Then, 120 µL of the sterile IV solution described in section 2.2 were injected in the lateral tail vein using an insulin syringe (27 G, 1.0 mL). Both administration routes allowed the administration of the same dose (8.33 mg/kg).

After the administration of lacosamide, animals were sacrificed by cervical dislocation followed by decapitation at predefined time points (5, 15, 30, 60, 90, 120, 240, 360 and 480 min, *n* = 5 per time point). Blood was immediately collected into heparinized tubes and tissues of interest (brain, lungs and kidneys) were excised, gently washed with sodium chloride 0.9% solution, dried with sterile compress and weighed. Blood was centrifuged at 4°C and 2880 *g* for 10 min, followed by plasma collection for further sample treatment and drug quantification (section 2.4.3). Using a THOMAS® Teflon tissue homogenizer, tissues were homogenized with 4 mL of sodium phosphate buffer (0.1 M, pH 5.0) per g of tissue.

All samples were stored at -80°C until appropriate treatment and subsequent chromatographic analysis.

2.4.3. Quantification of lacosamide in biological samples

The HPLC method to quantify lacosamide in plasma and tissues was adapted from the previously developed and validated technique in human plasma, with slight changes optimized for mice plasma and tissues analysis (Gonçalves et al., 2018).

Sample preparation consisted of adding 40 µL of methanol, 10 µL of antipyrine (50 µg/mL) and 1 mL of ethyl acetate to 100 µL of plasma or 150 µL of tissue homogenate supernatant. After vortex-mixing for 30 seconds and centrifugation at 12,045 *g* during 3 or 5 min for plasma or tissue homogenate, respectively, the organic phase was collected into a glass tube and the procedure was repeated. Organic phases were totally evaporated at 45°C under a slight nitrogen stream. The solid residue was reconstituted in 100 µL of water and acetonitrile (90:10, v/v), followed by 1 min of vortex-mixing and filtration through Costar® Spin-X® (0.22 µm, Corning, Inc., NY, USA) at 12,045 *g* for 3 or 5 min. A final volume of 20 µL of sample was injected into the HPLC system for lacosamide quantification.

A Shimadzu HPLC system (Shimadzu Corporation, Kyoto, Japan) equipped with a solvent release model (LC-20A), a degasser (DGU-20A5), an autosampler (SIL-20AHT), a column oven (CTO-10ASVP) and a diode array detector (SPD-M20A) were used. Control and monitoring of the apparatus, as well as result collection were performed by LCsolution Software (Shimadzu Corporation, Kyoto, Japan).

Lacosamide and the IS were separated in a LiChroCART® Purospher® Star C18 reversed-phase column (55 mm × 4 mm, 3 µm particle size; Merck KGaA, Darmstadt, Germany), at 40ºC, and employing, at 1 mL/min, the same elution gradient reported in (Gonçalves et al., 2018). Diode array detector was set at 220 nm.

A partial validation was performed in plasma, brain, lung and kidney according to the international guidelines of bioanalytical method validation of the European Medicines Agency and the Food and Drug Administration (EMA, 2011; FDA, 2018). The validation parameters (n=5) included selectivity, linearity, inter- and intra-day accuracy and precision, recovery and the results are summarized in **Table 1**. Aliquots (10 µl) of the working standard solutions of lacosamide were added to blank mice plasma and tissue homogenate to obtain seven calibration standards and four quality control (QC) samples. Calibration standards were used to assess linearity while the QCs were used to determine inter- and intra-day accuracy and precision as well as recovery. Descriptive statistics reported for the partial validation of HPLC bioanalytical method was performed using Microsoft Excel® 2016.

2.4.4. Pharmacokinetic and statistical analysis

For both administration routes, mean experimental concentration *versus* time profiles were plotted in plasma, brain, lung and kidney and submitted to non-compartmental pharmacokinetic analysis, using WinNonlin software, version 5.2 (Pharsight Co, Mountain View, CA, USA). The pharmacokinetic parameters were estimated considering the mean concentrations (n = 5) obtained at each post-dose time point and included the maximum concentration (C_{max}) of lacosamide achieved in plasma and tissues, the time required to reach C_{max} (t_{max}), the area under the concentration-time curve from time zero to the time of last measurable concentration (AUC_t), and from time zero to infinity (AUC_{inf}), which is calculated by the addition of AUC_t and the quotient between the last quantifiable concentration (C_{last}) and the apparent elimination rate constant (K_{el}). K_{el} is estimated by a log-linear regression of the terminal segment of the concentration-time profile. The area under the extrapolated curve [AUC_{extrap} (%)] was also estimated, representing the drug exposure since the last time for which the concentration was quantifiable to infinity, which should not exceed 20%. Additionally, the apparent elimination half-life ($t_{1/2}$), and the mean residence time (MRT) were also quantified. The aforementioned parameters allowed the calculation of the absolute bioavailability in accordance witth the equation 1 (Table 2).
Plasma-to-tissue ratios were also estimated to compare the affinity of lacosamide for each organ in relation to its systemic exposure.
In order to assess the tendency of lacosamide to reach the brain after IN administration, specific parameters regarding drug delivery were determined, namely the drug targeting efficiency (DTE), which predicts the drug propensity to be directly delivered from the nasal cavity to the brain and is calculated based on equation 2 **(Table 2)**. When expressed as a percentage, a DTE value higher than 100% suggests a preferential drug transport to the brain directly through the nasal cavity instead of the systemic route (Kumar et al., 2008; Nigam et al., 2019). In addition, direct transport percentage (DTP) was calculated according to equation 3 **(Table 2)**, which corresponds

to the drug percentage that reaches the brain by direct route (Fatouh et al., 2017). The brain bioavailability of lacosamide, which corresponds to the ratio between the AUC_t in brain after IN and IV administrations, was also estimated (equation 4, **Table 2**).

Graphpad Prism® 5.03 software (San Diego, CA, USA) was used to express the concentrations as mean ± standard error of the mean (SEM) and determine statistical differences between both administrations (IN and IV). Unpaired two-tailed Student's t-test was performed between IN and IV administration groups. Differences were considered statistically significant for *p*-values lower than 0.05 ($p < 0.05$).

3. Results

3.1. Cell viability of intranasal thermoreversible gel

The herein used IN gel was developed based on our previous investigations (Gonçalves et al., 2020; Gonçalves et al., 2019; Serralheiro et al., 2015), maintaining the basis of Pluronic F-127 block copolymer due to its physicochemical and biological properties, namely its thermoreversibility in water (Gonçalves et al., 2020; Gonçalves et al., 2019). This means that it is liquid at room temperature and gelifies at the temperature of nasal mucosa.

RPMI 2650 cells were incubated for 24 h with distinct gel formulations, firstly empty and then loaded with lacosamide at different concentrations. Their effects on cell viability in relation to the control group are expressed in **Figure 1**. Accordingly, it is evident that, although no differences have been registered, inclusion of lacosamide in Carbopol 974P and polycarbophil gels slightly decreased cell viability in relation to the correspondent unloaded gel. Moreover, cell viability was always equal to or higher than 85%, with exception of the Carbopol 974P gel loaded with lacosamide at the highest concentration (mean value of 83.75%) and polycarbophil gel loaded with lacosamide at 50, 100 and 150 µM (mean values of 82.72%, 81.53% and 80.31%, respectively).

It was also observed that at the concentration range herein investigated (1-400 µM, **Figures 1 and 2**), lacosamide did not affect the viability of RPMI 2650 cells, although it decreases as concentrations increase. No statistically significant differences were observed. Similar results were also found in Calu-3 lung cells between 1 and 100 µM (Figure 2).

3.2. *In vivo* pharmacokinetic analysis

The mean lacosamide concentrations and SEM (*n* = 5) obtained at each time-point in plasma, brain, lungs and kidneys after single dose administration of lacosamide (8.33 mg/kg) by IV and IN routes to mice are depicted in **Figure 3** together with the statistical differences. The correspondent pharmacokinetic parameters are presented in **Table 3**.

The C_{max} of lacosamide in plasma was attained at 5 min for both routes of administration even though it was significantly higher after IV injection (12.67±1.429 µg/mL) than IN instillation (8.59±0.464 µg/mL). At the remaining time-points, profiles were practically overlapped with exception of 90 and 240 min, which revealed statistically higher concentrations after IN administration (p<0.01 and p<0.05, respectively, **Figure 3A**). Nonetheless, systemic exposure was slightly higher for the IN gel (850.33 µg.min/mL *vs* 705.93 µg.min/mL), probably because its clearance was slower, as suggested by the enhanced $t_{1/2}$ (96 min *vs* 34 min) and MRT (139 min *vs* 60 min, **Table 3**). These facts are corroborated by the enhanced values observed for the K_{el} (0.0072 min^{-1} *versus* 0.0206 min^{-1} for IN and IV routes, respectively).

Regarding brain tissue, C_{max} of lacosamide was attained at 15 min for both administration routes, but lower values were found after IN administration (3.45 µg/g *vs* 4.79 µg/g), with statistical differences (p<0.05). Interestingly, the mean concentration attained at 5 min post IV dosing was approximately twice of that achieved after IN instillation (2.354±0.282 µg/g and 1.467±0.101 µg/g, **Figure 4B**), even though the differences were not statistically significant. The remaining time-points clearly evidence that lacosamide concentrations are higher after IN administration (**Figure 4B**), culminating in a considerably higher brain exposure to lacosamide (given by the AUC_{inf}) following IN administration (471.84 µg.min/mL *vs* 289.36 µg.min/mL, **Table 3**). Moreover, the brain-to-plasma ratios were small and similar for both routes (**Table 3**). Notwithstanding, DTE was 128.67% and DTP was 22.28%.

Regarding the concentration-time profile obtained for lung tissue after IV injection (**Figure 3C**), lacosamide concentrations were always inferior to the LLOQ of the analytical technique with exception of 15 min post-administration (mean value of 2.52±1.03 µg/g). After IN instillation of lacosamide loaded gel, the drug was quantified at 5, 15 and 30 min and attained a C_{max} value of 6.65±1.11 µg/g. Importantly, this value is lower than those tested *in vitro* in Calu-3. In lungs, the estimated DTE value was 888.91%, confirming that there is direct passage to the lungs even though lacosamide is quickly eliminated, presenting unquantifiable concentrations after 30 min post-administration.

In the kidney, lacosamide concentrations were also higher only at initial sample collection times (5 and 15 min) after IN dosing; thereafter, IV concentrations were higher, attaining statistically significant differences at 60 min post-dosing (**Figure 3D**). Complementarily, kidney exposure to lacosamide was considerably higher for the IV route (762.61 µg.min/mL *vs* 357.56 µg.min/mL), which is corroborated by the higher $AUC_{kidney}/AUC_{plasma}$ ratio (0.51 *vs* 0.42) and the DTE value of 38.92%.

Discussion

Lacosamide is undeniably effective in epilepsy, particularly due to its anticonvulsant and anti-epileptogenic effects. It is also demonstrating success in other neurological diseases as antinociceptive. In addition, its IV administration is considered essential when it is not possible to use the oral route. However, IV injection is invasive and requires health care professionals to be performed. Therefore, developing a novel non-invasive therapeutic strategy to deliver lacosamide into the brain is expected to increase its clinical use, adherence to therapy and marketing potential.

Making use of our previous *know-how* in nose-to-brain delivery, this study is the first to demonstrate the potential of the IN route to deliver lacosamide into the brain.

Herein a simple *in situ* mucoadhesive gel system was used to counterbalance the anatomical and physiological characteristics of nasal mucosa, particularly the fast mucociliary clearance and efflux transporters of the nasal cavity that reduce drug absorption. Therefore, Pluronic F-127 was selected at the concentration of 22.5% (w/v). Besides its already well-documented thermoreversibility (Gonçalves et al., 2020; Gonçalves et al., 2019), it is a long poly(propylene)oxide block with high hydrophobicity that allows the incorporation of lipophilic compounds such as lacosamide. Furthermore, it strongly modifies the microviscosity of plasma membranes and potentially inhibits P-gp (Pitto-Barry and Barry, 2014), which is strongly expressed in the nasal mucosa of mice, rats and humans (Oliveira et al., 2016). Bearing in mind that lacosamide is a P-gp substrate, inhibition of this efflux transporter by Pluronic F-127 is expected to increase lacosamide distribution from the nasal mucosa to the brain. Carbopol 974P and Noveon® Polycarbophil (0.2%, w/v) were tested together with Pluronic F-127 to increase gel viscosity and avoid quick drug clearance from the nasal cavity towards the nasopharyngeal region by prolonging its retention time in the nasal cavity. Since the gel system composed of Noveon® Polycarbophil and Pluronic F-127 when loaded with lacosamide compromised the viability of RPMI 2650 cells to values lower than 85 % (**Figure 1**), the Carbopol 974P plus Pluronic F-127 combination was selected for IN administration to mice. It is important to note that maximum concentrations tested *in vitro* were defined in accordance with drug solubility in DMSO, since this should not exceed 0.5%. Nevertheless, herein, the DMSO percentage did not exceed 0.2%.

When the IN formulation was optimized, a comparative pharmacokinetic study was performed in mice after IN or IV administration of lacosamide at the same dose (8.33 mg/kg). Based on the Assessment Report of Vimpat® (EMA, 2008), lacosamide revealed to be effective at the dose of 1 mg/kg in a mouse model essential tremor and it completely antagonized tonic convulsions with no adverse effects at 20 mg/kg. Therefore, we tested different IV doses between 1 and 20 mg/kg and selected the 8.33 mg/kg dose because it led to plasma concentrations that were within the therapeutic range

suggested for lacosamide (2.2-20 μg/mL) in therapeutic drug monitoring (Schultz and Mahmoud, 2020).

The pharmacokinetic results demonstrated that, similarly to IV injection, the IN instillation of lacosamide *in situ* nasal gel brought an extensive but longstanding systemic absorption of the drug, attaining C_{max} at the same time, although with lower values than IV route. The absolute bioavailability value achieved for intranasally administered lacosamide was high (120.40%). This value is superior to 100% presumably because of the inter-individual variability among different animals since each mouse was assigned not only for one of the two administration groups but also to a unique sampling time-point. Nevertheless, it illustrates the fact that a substantial drug fraction is absorbed from the nasal cavity into the systemic circulation, gaining access to the CNS by crossing the BBB.

Moreover, the same t_{max} value was found in brain (15 min) after IN and IV administration, suggesting a fast delivery of lacosamide to the brain. The DTE was 128.67%, indicating that lacosamide is directly delivered from the nose to the brain. Approximately 22.28% of the drug reached the brain by direct nose-to-brain pathways, probably through the olfactory and trigeminal nerves. This means that IN delivery may be very practical and useful in emergencies. Furthermore, after the first 15 min, brain concentrations were always higher for IN administration, suggesting a sustained drug release from the nasal system and/or a slow absorption into the systemic circulation following its passage through the BBB to the target. These findings, together with the higher K_{el} and smaller MRT and $t_{1/2}$ of lacosamide in the brain following IV injection, suggest that a longer protective effect may occur with the IN instillation. Also, IN dosing may require a less frequent administration than IV or oral administrations.

Even though plasma concentrations were similar between both routes of administration, anticipating similar peripheral side effects, the lower drug exposure in renal tissue must be highlighted. Indeed, C_{max} is reached earlier after IN administration, but it is smaller, as well as the extent of drug exposure given by AUC_t, which is approximately 50% of that observed after IV injection. This feature may become relevant for patients with renal failure for whom lacosamide prescription has several limitations, as discussed in section 1. Since the renal concentrations achieved after IN dosing do not exceed the C_{max} reported for IV route, less toxicity is expected to occur.

Kidneys have a different pharmacokinetic profile compared to lungs. This can be justified because lacosamide is excreted by renal route and one of its major adverse effects regards the kidney. Therefore, it probably reaches the kidney earlier and at higher quantities than those attained in the lung. Moreover, to the best of our knowledge, no pulmonary adverse effects have been reported for lacosamide probably due to its low distribution to the lungs. However, the DTE is 888%, which clearly emphasizes the direct nose-to-lung delivery of lacosamide, even though the lung-to-plasma ratio was the lowest when compared

with other organs. This means that lacosamide has higher affinity to brain and kidneys than to lungs. On the other hand, it is important to highlight that lacosamide was detected at all the time-points but it was only quantified 15 min after its IV administration. After IN administration, lacosamide was quantifiable up to 30 min. This means that a slight increase in AUC after IN instillation comparatively to IV route is sufficient to significantly increase DTE. Moreover, the *in vitro* investigations herein performed with Calu-3 cells evidence that lacosamide does not compromise cell viability including at concentrations higher than those found *in vivo*. These results are in accordance with pharmacokinetic studies that evaluated the nose-to-brain delivery of levetiracetam (Gonçalves et al., 2019) and zonisamide (Gonçalves et al., 2020). Nevertheless, the reported DTE (888%) is considerably higher than those of levetiracetam (253.63%) or zonisamide (144.47%) (Gonçalves et al., 2020; Gonçalves et al., 2019). In opposition, the DTE into the brain was higher for levetiracetam [182.35% (Gonçalves et al., 2019)] and zonisamide [149.54% (Gonçalves et al., 2020)] than for lacosamide (128.67%). These findings can be justified not only because of the different physicochemical characteristics of the drugs [eg. levetiracetam has the lowest partition coefficient (logP = -0.6), followed by zonisamide (logP = 0.5) and lacosamide (logP = 0.7)] but also because of the nasal device that was used. Herein, catheter was used for the administration of lacosamide, instead of the pulverization system used for the nasal instillation of levetiracetam and zonisamide (Gonçalves et al., 2020; Gonçalves et al., 2019). These results alert the scientific community for the impact of drug physicochemical characteristics and nasal device when designing future nasal formulations.

Conclusion

To the best of our knowledge, a comprehensive characterization of the pharmacokinetic profiles of lacosamide in plasma, brain, lungs and kidneys following IN instillation to mice was herein reported for the first time.

Altogether, IN and IV administrations of lacosamide exhibited similar concentration–time profiles, suggesting similar pharmacological responses. However, brain drug exposure was enhanced after IN instillation, demonstrating, together with a DTE of 128.67% and a DTP of 22.28%, the direct drug delivery from the nasal cavity to the brain. Moreover, t_{max} in brain was similar for both administration routes (15 min), highlighting the potential of IN delivery for acute convulsive emergencies. The MRT value of lacosamide in the brain supports the sustained concentrations and the usefulness of IN administration during chronic treatments with lacosamide.

The IN instillation of lacosamide loaded in the mucoadhesive gel is practical and adequate to be used outside the hospital setting particularly due to its ease and reduced frequency of administration, as well as improved patient compliance and comfort. Herein, evidence was gathered accounting for a direct transport of lacosamide from the nose to the brain, circumventing the BBB, which may render the

IN route as a promising and valuable drug delivery strategy for a prospective management of pharmacoresistance.

Acknowledgments

The authors acknowledge Fundo Europeu de Desenvolvimento Regional (FEDER) funds through Portugal 2020 in the scope of the Operational Program for Competitiveness and Internationalization, and Fundação para a Ciência e Tecnologia (FCT) I.P./MCTES, Portuguese Agency for Scientific Research, through national funds (PIDDAC) within the scope of the research project CENTRO-01-0145-FEDER-03075 and POCI-01-0145-FEDER-030478.

Figure Captions

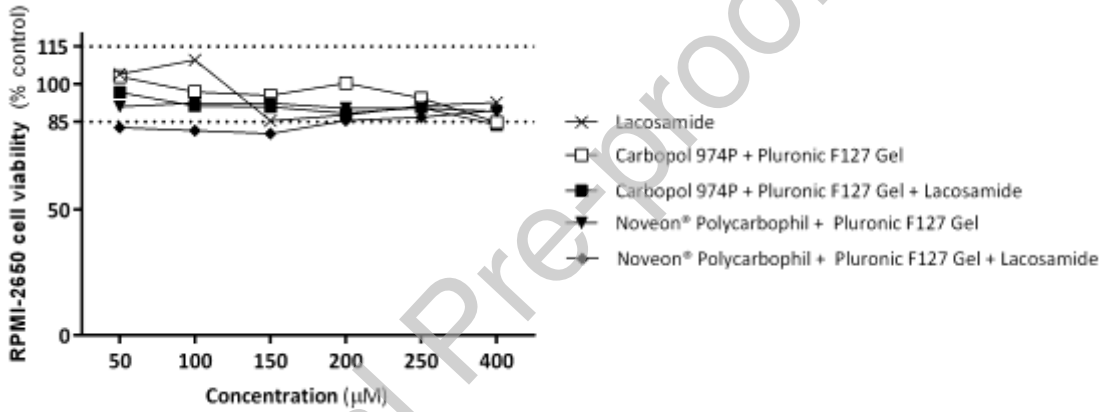

Figure 1 – Viability (%) of RPMI-2650 cells after incubation with lacosamide, empty Noveon® Polycarbophil and Carbopol® thermoreversible gels, and thermoreversible gels loaded with lacosamide at the same concentrations, for 24 h (50, 100, 150, 200, 250 and 400 μM). Data represented as mean ± standard deviation (*n* = 4).

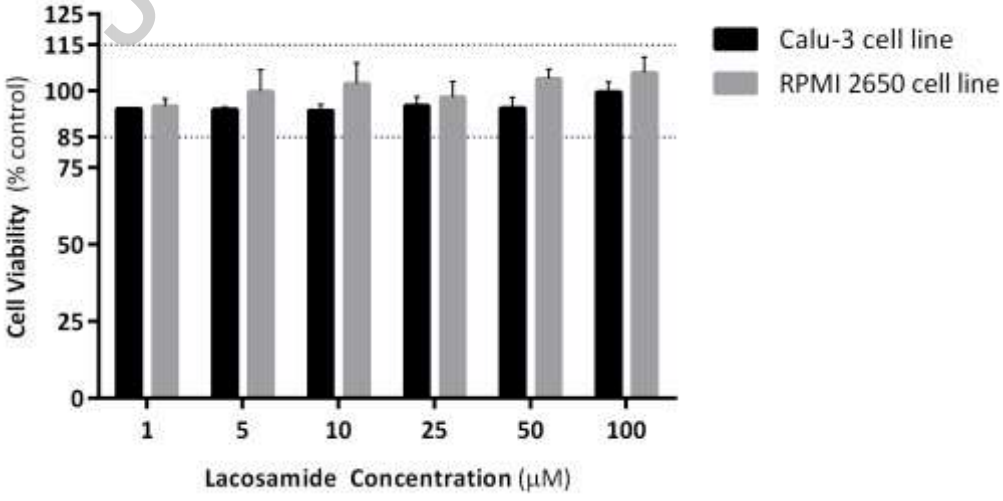

Figure 2 – Viability (%) of Calu-3 and RPMI 2650 cells after incubation with lacosamide for 24 h (1-100 µM). Data represented as mean ± standard deviation (*n* = 4).

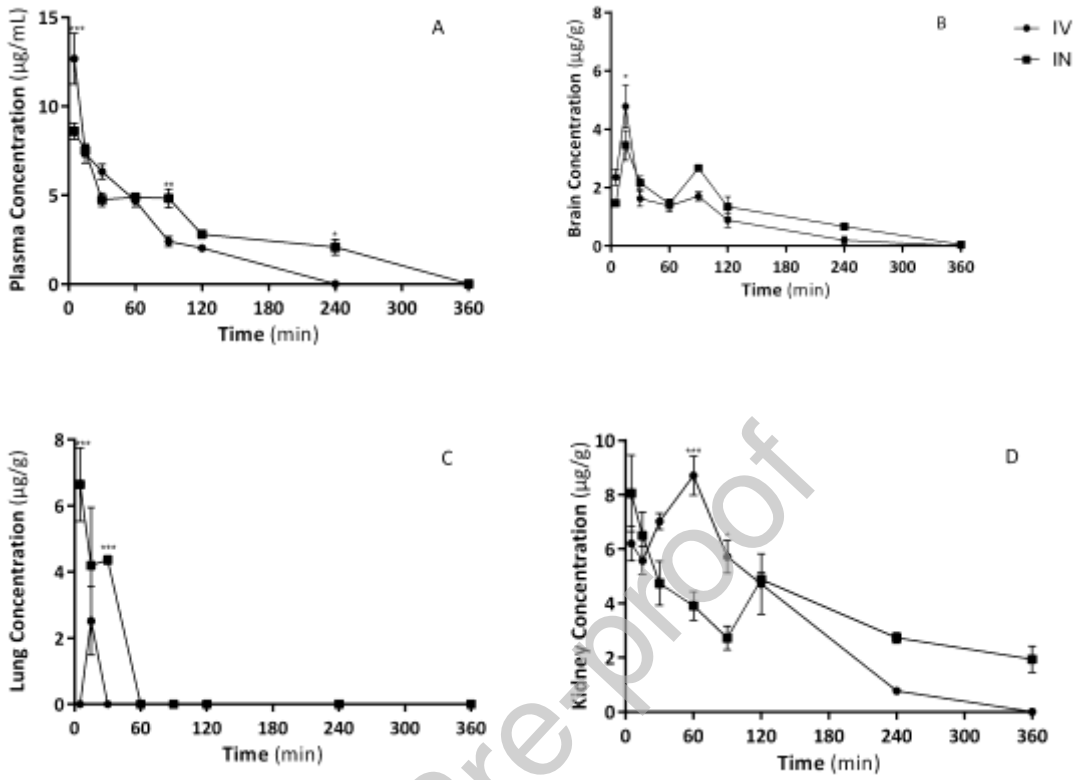

Figure 3 – Concentration-time profiles of lacosamide after intranasal (IN) and intravenous (IV) administration (8.33 mg/kg) in plasma (A), brain (B), lung (C) and kidney (D). The symbols represent the mean ± SEM values of five determinations per time point (*n* = 5). * $p<0.05$

CREDIT AUTHOR STATEMENT

Manuscript ID: PHASCI-S-20-02119

Joana Gonçalves: Investigation; Formal analysis; Methodology; Visualization; Writing - Original Draft

Gilberto Alves: Formal analysis; Writing - Review & Editing; Supervision;

Carla Fonseca: Investigation

Andreia Carona: Investigation

Joana Bicker: Supervision; Writing - Review & Editing

Amílcar Falcão: Formal analysis; Funding acquisition

Ana Fortuna: Conceptualization; Methodology; Formal analysis; Writing - Review & Editing; Supervision; Project administration; Funding acquisition

References:

Al-Massri KF, Ahmed LA and El-Abhar HS (2018) Pregabalin and lacosamide ameliorate paclitaxel-induced peripheral neuropathy via inhibition of JAK/STAT signaling pathway and Notch-1 receptor. *Neurochem Int* **120**:164-171.

Amengual-Gual M, Ulate-Campos A and Loddenkemper T (2019) Status epilepticus prevention, ambulatory monitoring, early seizure detection and prediction in at-risk patients. *Seizure* **68**:31-37.

Carmland ME, Kreutzfeldt M, Holbech JV, Andersen NT, Jensen TS, Bach FW, Sindrup SH and Finnerup NB (2019) Effect of lacosamide in peripheral neuropathic pain: study protocol for a randomized, placebo-controlled, phenotype-stratified trial. *Trials* **20**:019-3695.

Cawello W, Fuhr U, Hering U, Maatouk H and Halabi A (2013) Impact of impaired renal function on the pharmacokinetics of the antiepileptic drug lacosamide. *Clin Pharmacokinet* **52**:897-906.

Cawello W, Mueller-Voessing C and Fichtner A (2014) Pharmacokinetics of lacosamide and omeprazole coadministration in healthy volunteers: results from a phase I, randomized, crossover trial. *Clin Drug Investig* **34**:317-325.

de Biase S, Gigli GL, Valente M and Merlino G (2014) Lacosamide for the treatment of epilepsy. *Expert Opin Drug Metab Toxicol* **10**:459-468.

Dean L (2018) Lacosamide Therapy and CYP2C19 Genotype Drug : Lacosamide The Cytochrome P450 Superfamily. *Medical Genetics Summaries [Internet]*.

EMA (2008) Assessment report for Vimpat - Procedure No. EMEA/H/C/000863

EMA (2011) Guideline on bioanalytical method validation - EMEA/CHMP/EWP/192217/2009 Rev. 1 Corr. 2**, ((CHMP) CfMPfHU ed).

Engel J, Jr. and Pitkänen A (2020) Biomarkers for epileptogenesis and its treatment. *Neuropharmacology* **167**:1.

Fatouh AM, Elshafeey AH and Abdelbary A (2017) Intranasal agomelatine solid lipid nanoparticles to enhance brain delivery: formulation, optimization and in vivo pharmacokinetics. *Drug Des Devel Ther* **11**:1815-1825.

FDA (2018) Bioanalytical Method Validation Guidance for Industry.

Gonçalves J, Alves G, Bicker J, Falcão A and Fortuna A (2018) Development and full validation of an innovative HPLC-diode array detection technique to simultaneously quantify lacosamide, levetiracetam and zonisamide in human plasma. *Bioanalysis* **10**:541-557.

Gonçalves J, Alves G, Carona A, Bicker J, Vitorino C, Falcão A and Fortuna A (2020) Pre-Clinical Assessment of the Nose-to-Brain Delivery of Zonisamide After Intranasal Administration. **37**:74.

Gonçalves J, Bicker J, Gouveia F, Liberal J, Oliveira RC, Alves G, Falcão A and Fortuna A (2019) Nose-to-brain delivery of levetiracetam after intranasal administration to mice. *Int J Pharm* **564**:329-339.

Halford JJ and Lapointe M (2009) Clinical perspectives on lacosamide. *Epilepsy Curr* **9**:1-9.

Kim GH, Byeon JH and Eun BL (2017) Neuroprotective Effect of Lacosamide on Hypoxic-Ischemic Brain Injury in Neonatal Rats. *J Clin Neurol* **13**:138-143.

Kumar B, Modi M, Saikia B and Medhi B (2017) Evaluation of Brain Pharmacokinetic and Neuropharmacodynamic Attributes of an Antiepileptic Drug, Lacosamide, in Hepatic and Renal Impairment: Preclinical Evidence. *ACS Chem Neurosci* **8**:1589-1597.

Kumar M, Misra A, Babbar AK, Mishra AK, Mishra P and Pathak K (2008) Intranasal nanoemulsion based brain targeting drug delivery system of risperidone. *Int J Pharm* **358**:285-291.

Lazarowski A, Czornyj L, Lubienieki F, Girardi E, Vazquez S and D'Giano C (2007) ABC transporters during epilepsy and mechanisms underlying multidrug resistance in refractory epilepsy. *Epilepsia* **48 Suppl 5**:140-149.

Leandro K, Bicker J, Alves G, Falcão A and Fortuna A (2019) ABC transporters in drug-resistant epilepsy: mechanisms of upregulation and therapeutic approaches. *Pharmacological research* **144**:357-376.

Lionetto L, Negro A, Palmisani S, Gentile G, Del Fiore MR, Mercieri M, Simmaco M, Smith T, Al-Kaisy A, Arcioni R and Martelletti P (2012) Emerging treatment for chronic migraine and refractory chronic migraine. *Expert Opin Emerg Drugs* **17**:393-406.

Moutal A, Chew LA, Yang X, Wang Y, Yeon SK, Telemi E, Meroueh S, Park KD, Shrinivasan R, Gilbraith KB, Qu C, Xie JY, Patwardhan A, Vanderah TW, Khanna M, Porreca F and Khanna R (2016) (S)-lacosamide inhibition of CRMP2 phosphorylation reduces postoperative and neuropathic pain behaviors through distinct classes of sensory neurons identified by constellation pharmacology. *Pain* **157**:1448-1463.

Nigam K, Kaur A, Tyagi A, Nematullah M, Khan F, Gabrani R and Dang S (2019) Nose-to-brain delivery of lamotrigine-loaded PLGA nanoparticles. *Drug Deliv Transl Res* **9**:879-890.

Oliveira P, Fortuna A, Alves G and Falcao A (2016) Drug-metabolizing Enzymes and Efflux Transporters in Nasal Epithelium: Influence on the Bioavailability of Intranasally Administered Drugs. *Curr Drug Metab* **17**:628-647.

Page B, Page M and Noel C (1993) A new fluorometric assay for cytotoxicity measurements in-vitro. *Int J Oncol* **3**:473-476.

Pitto-Barry A and Barry N (2014) Pluronic® block-copolymers in medicine: from chemical and biological versatility to rationalisation and clinical advances. *Plolymer Chemistry* **5**:7.

Rampersad SN (2012) Multiple applications of Alamar Blue as an indicator of metabolic function and cellular health in cell viability bioassays. *Sensors* **12**:12347-12360.

Rizzo A, Donzelli S, Girgenti V, Sacconi A, Vasco C, Salmaggi A, Blandino G, Maschio M and Ciusani E (2017) In vitro antineoplastic effects of brivaracetam and lacosamide on human glioma cells. *J Exp Clin Cancer Res* **36**:017-0546.

Schultz L and Mahmoud SH (2020) Is Therapeutic Drug Monitoring of Lacosamide Needed in Patients with Seizures and Epilepsy? *Eur J Drug Metab Pharmacokinet* **45**:315-349.

Serralheiro A, Alves G, Fortuna A and Falcão A (2015) Direct nose-to-brain delivery of lamotrigine following intranasal administration to mice. *Int J Pharm* **490**:39-46.

Wang GX, Wang DW, Liu Y and Ma YH (2016) Intractable epilepsy and the P-glycoprotein hypothesis. *Int J Neurosci* **126**:385-392.

Wang X, Yu Y, Ma R, Shao N and Meng H (2018) Lacosamide modulates collapsin response mediator protein 2 and inhibits mossy fiber sprouting after kainic acid-induced status epilepticus. *Neuroreport* **29**:1384-1390.

Zachari MA, Chondrou PS, Pouliliou SE, Mitrakas AG, Abatzoglou I, Zois CE and Koukourakis MI (2013) Evaluation of the alamarblue assay for adherent cell irradiation experiments. *Dose Response* **12**:246-258.

Zhang C, Chanteux H, Zuo Z, Kwan P and Baum L (2013) Potential role for human P-glycoprotein in the transport of lacosamide. *Epilepsia* **54**:1154-1160.

Table 1. Validation parameters of the analytical method developed in high performance liquid chromatography (HPLC-DAD) for quantification of lacosamide in plasma and brain, lung and kidney
homogenate (*n = 5*).

n er	Plasma	Brain	Lungs	Kidneys
on range[a]	0.5 - 30	0.4 - 120[b]	4 - 120[b]	4 – 120[b]
on a	y=0.0924x - 0.0353	y=0.0557x + 0.0123	y=0.0500x – 0.009	y=0.0497x + 0.09
nt of ation (r^2)	0.996	0.997	0.995	0.995
/mL)	0.5	0.1	1	1
on (%CV)	5.84 - 10.69	2.24 – 14.00	1.79 – 8.69	1.82 – 12.76
cy (%Bias)	-8.40 – 6.65	-3.03 – 10.99	-1.07 - 8.25	-1.29 – 7.18
on (%CV)	5.90 - 7.80	2.74 – 11.55	1.25 – 4.88	6.36 – 9.87
cy (%Bias)	-5.50 - 9.74	-9.47 – 9.69	-5.71 – 7.72	1.06 – 9.73
(%)	83.93 – 96.25	82.70 - 90.11	86.91 – 95.52	89.05 - 97.45

[a] Inter-day values (n = 5) and the equation of the calibration curve is given by the general equation of $y = mx+b$, with *m* corresponding to the slope and *b* to the intercept. The equation represents the peak areas signals of each drug to that of the internal standard (*y*), versus the corresponding plasma concentration of lacosamide (x).

[b] values expressed in µg/g.

CV, coefficient of variation; Bias, deviation from nominal value; LLOQ, lower limit of quantification.

Table 2. Equations for determination of bioavailability and drug delivery parameters described in section 2.4.4.

Equation 1	$\mathbf{F = \frac{AUC_{t\,IN}}{AUC_{t\,IV}} \times 100}$
Equation 2	$\mathrm{DTE\ (\%)} = \frac{(AUC_{brain}/AUC_{plasma})_{IN}}{(AUC_{brain}/AUC_{plasma})_{IV}} \times 100$
Equation 3	$\mathrm{DTP\ (\%)} = \frac{\mathrm{AUC_{brain\ IN}} - \left[\frac{\mathrm{AUC_{brain\ IV}}}{\mathrm{AUC_{plasma\ IV}}}\ \mathrm{x}\ \mathrm{AUC_{plasma\ IN}}\right]}{\mathrm{AUC_{brain\ IN}}} \mathrm{x}\ 100$
Equation 4	$\mathrm{B_{brain\ IN/IV}} = \frac{\mathrm{AUC_{brain\ IN}}}{\mathrm{AUC_{brain\ IV}}}$

AUC_t, area under drug concentration-time curve from time zero to the time of last measurable concentration; $B_{brainIN/IV}$, brain bioavailability between IN and IV routes; DTE, drug targeting efficiency; DTP, direct transport percentage; F, bioavailability; IN, intranasal, IV, intravenous.

Table 3. Pharmacokinetic parameters following administration of lacosamide (8.33 mg/kg) in plasma and tissue (brain, lung and kidney) of mice through intranasal thermoreversible gel (IN) and intravenous solution (IV).

Pharmacokinetic Parameters[a]	**Plasma**		**Brain**		**Lung**		**Kidney**	
	IN	IV	IN	IV	IN	IV	IN	IV
t_{max} (min)	5.00	5.00	15.00	15.00	5.00	15.00	5.00	60.00
C_{max} (µg/mL)[b]	8.59	12.67	3.45[b]	4.79[b]	6.65[b]	2.52	7.33	8.70
AUC_t (µg.min/mL)	850.33	705.93	425.44[c]	274.49[c]	135.02[c]	12.61	357.56	762.61
AUC_{inf} (µg.min/mL)	1044.33	711.77	471.84	289.36	420.70[c]	ND	ND	1028.18
AUC_{extrap} (%)	18.58	0.82	9.83	5.14	67.90	ND	ND	25.83
k_{el} (min^{-1})	0.0072	0.0206	0.0063	0.0134	0.0153	ND	ND	0.0141
$t_{1/2}$ (min)	96	34	109	52	45	ND	ND	29
MRT (min)	139	60	156	81	70	ND	ND	92
F (%)[d]	120.46	-	-	-	-	-	-	-
AUC_t Ratios	**IN**	**IV**	**DTE (%)**	**DTP (%)**				
AUC_{brain}/AUC_{plasma}	0.50	0.39	128.67	22.28 %				
AUC_{lung}/AUC_{plasma}	0.16	0.02	888.91					
$AUC_{kidney}/AUC_{plasma}$	0.42	0.51	38.92					

[a] Parameters were estimated using the mean concentration-time profiles obtained from five different animals per time point (n = 5). [b] Values expressed in µg/g; [c] Values expressed in µg.min/g; [d] Absolute intranasal bioavailability (F) was calculated based on AUC_t values; AUC_{extrap}, Extrapolated area under the drug concentration time-curve; AUC_{inf}, Area under the concentration time-curve from time zero to infinite; AUC_t, Area under the concentration time-curve from time zero to the last quantifiable drug concentration; C_{max}, Maximum concentration; DTE, Drug targeting efficiency index; DTP, direct transport percentage; k_{el}, Apparent elimination rate constant; MRT, Mean residence time; NC, not calculated; $t_{1/2}$, Apparent terminal elimination half-life; t_{max}, Time to achieve the maximum peak concentration.

Graphical Abstract